APPLICATIONS OF BEHAVIORAL MODELING AND SIMULATION ON LAB-ON-A-CHIP: MICRO-MIXER AND SEPARATION SYSTEM

Y. Wang
Department of Mechanical Engineering
Carnegie Mellon University
Pittsburgh, U.S.A., 15213
yiw@andrew.cmu.edu

Q. Lin
Department of Mechanical Engineering
Carnegie Mellon University
Pittsburgh, U.S.A., 15213
qlin@andrew.cmu.edu

T. Mukherjee
Department of Electrical and Computer Engineering
Carnegie Mellon University
Pittsburgh, U.S.A., 15213
tamal@ece.cmu.edu

ABSTRACT

This paper presents a behavioral modeling methodology and composable system simulation framework for elecrokinetic lab on a chip (LOC), especially on the micro-mixing and electrophoretic separation systems, using an analog hardware description language (Verilog-A). The developed models describe not only the behavior of individual components, but also the interactions between them. Both DC and transient analysis are performed in the framework. The accuracy (relative error less than 5%) and tremendous speedup (10~10,000×) of composable system simulations are verified by comparison to experiment and numerical studies.

1. INTRODUCTION

Lab on a chip (LOC) has been widely studied in the past decade, and hold great promise for a wide spectrum of applications in biology, medicine and chemistry [1, 8] that generally involve chemical analysis with other bioprocessing functionalities such as sample preparation, mixing, reaction, injection, separation analysis and detection. Figure 1 shows a schematic of a typical LOC, which consists of four subsystems: micro-mixer, reactor, injector and separation system. The operation of the entire LOC involves two stages. At the first stage, a voltage is applied between reservoirs 1, 2, 3, 4 and 5. The sample is moved by electrokinetic flow [10] under electric field and then diluted by buffer solvent or mixed with reagent (or enzyme) within the micro-mixer. The mixture then flows into reactor for chemical or bio-chemical reactions where external activations such as heat, light or catalyst might be needed. At the end of reactor, appropriate voltages could be exerted on reservoirs 6 and 7 to pinch and form a narrow product (or called analyte hereon) stream. Usually sample and reagent are continuously supplied by the reservoirs; therefore concentrations of all sample, reagent and analyte in the mixer and reactor at this stage are in steady state. After that, the operation enters the second stage, in which the voltage is switched on reservoirs 8 and 9; thus a band of the analyte is injected into the separation channel for further analysis. Because the analyte is composed of distinct charged species that migrate at different speeds under the electric field and eventually they can be separated, which is called electrophoretic separation; and the analyte concentration during this process is transient.

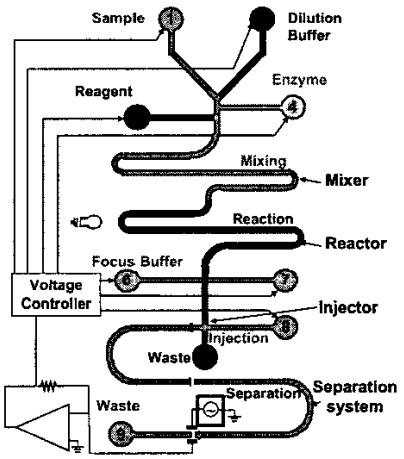

Figure 1. A schematic of a typical Lab-on-a-Chip.

Although LOC has advantages such as tremendous analysis speedup, parallel process and high integration and automation, efficient simulations for design at the system-level continue to be a challenge. This is due to the lack of CAD tools that consider the microfluidic interactions among subsystems and model the micro-scale physics that cause detrimental effects to LOC performance. Examples include turn geometry induced skew and broadening (dispersion) of the analyte band and the slow molecular diffusion-based mixing. Experimental trial-and-error, numerical computation methods and bottom-up design approaches can lead to unacceptably long design cycles. To address these issues, we will demonstrate the applications

of behavioral modeling and simulation for LOC. Examples will focus on the micro-mixer and separation system that can work as independent microfluidic devices or serve as a subsystem in an integrated LOC.

This paper presents a composable system simulation framework using an analog hardware description language (Verilog-A) integrating behavioral models of separation system [11] and micro-mixer [12] that are capable of capturing the effects of chip topology, sample/analyte-buffer properties on mixing and separation performance. Thus, it is generally applicable to the design of practical micro-mixing and separation devices.

2. COMPOSABLE SYSTEM SIMULATION

Our composable simulation framework consists of model libraries and simulation engine. One major contribution over [11, 12] is the development of Verilog-A libraries composed of parameterized behavioral models for commonly used elements in micro-mixing and separation systems. Users can compose a complex design schematic by wiring these blocks for a fast and reliable top-down iterative approach to system-level design.

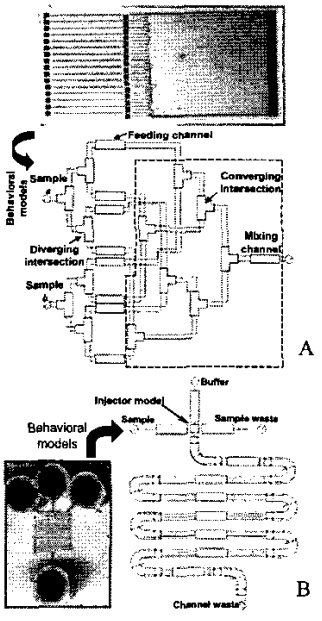

Figure 2. A multi-stream micro-mixer [7] (A) and a serpentine electrophoretic separation microchip [4] (B) and their schematics with analog hardware description behavioral models

Figure 2A illustrates a multi-stream micro-mixer [7] and its schematic, which consists of reservoirs, straight channels, and diverging and converging intersections. In the schematic, different samples *a* and *b* in two reservoirs are branched by diverging intersections into multiple streams, which are then transported by feeding channels and aligned alternately by cascade converging intersections to form an inter-digitated concentration profile at the inlet of the mixing channel, in which they eventually mix with each other (for figure clarity, we only shows eight streams and the photo only shows the parts enclosed by dashed line in the schematic). Figure 2B shows a serpentine separation system [4], which is decomposed into a series of elements including reservoirs, detector, injector, straight channels and turns. These elements are then linked via interface parameters according to the spatial layout and physics. Cadence [13] is used to netlist the structure of the composable network and Spectre [13] is employed as the simulator in this paper.

2.1 Interface parameters

The first step in creating a composable model of a system is to identify the parameters that will be communicated between neighboring elements (interface parameters). There are two kinds of interface parameters involved in the network. One is the nodal voltage globally determined by Ohm's and Kirchhoff's laws, which applies to all subsystems in an electrokinetic LOC. The other pertains to the corresponding microfluidic physics in the individual device. For example, within the micro-mixer, different samples or reagents carried by electrokinetic flow mix with each other and their concentrations stay steady-state. Thus the microfluidic interface parameters only include concentration coefficients (d_n), the Fourier series coefficient of the widthwise concentration profile. But for the electrophoretic separation system, the concentration of the injected analyte band is transient and band spreads out (dispersion) as it moves downstream; and hence the interface parameters include variance (σ^2), the longitudinal standard deviation of the cross-sectional average concentration; skew coefficients (B_n), used to describe the skew caused by the turns; separation time (t), the moment the center of mass of the band reaches the element; and amplitude (A), the maximum concentration. All these microfluidic interface parameters are associated with multiple samples or species of the analyte, thus wiring busses are used to connect between schematic elements. In addition, since changes to these parameters occurring in the downstream elements do not affect the upstream values, they are calculated using a directional signal flow in which the output from one element is assigned as the input to the next.

2.2 Behavioral models

After selecting the interface parameters, the second step of developing a composable model library is selecting the list of composable elements and deriving behavioral models

for each element. As discussed above, depending on the microfluidic physics of different devices, the contents of the libraries are different. The micro-mixer library has eight elemental models, which are reservoirs, straight channel, turns (90° or 180°, clockwise or counter-clockwise), diverging and converging intersections. The separation system library includes seven basic models: turns (90° or 180°, clockwise or counter-clockwise), straight channel, injector and detector.

The goal of each behavioral model is to capture the input-output signal flow relationship between the microfluidic interface parameters and the equivalent Kirchhoffian electric network for the voltage interface parameter (see Figure 3). In a simulation scheme, the steady nodal voltage and the electric field through the element will be determined first. Users only need to input the voltages applied on all reservoirs as boundary conditions, and the simulator is able to calculate the nodal voltage distribution, which is another new feature beyond [11, 12]. Based on the computed electric field (E), the input-output functions of the microfluidic interface parameters are then calculated.

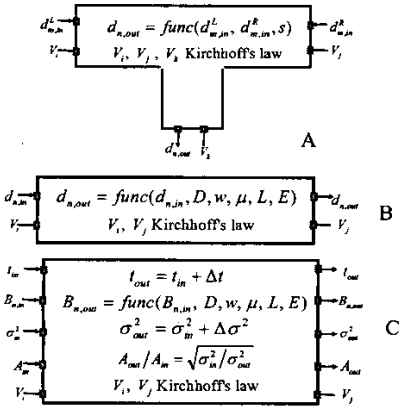

Figure 3. Structures of the behavioral models for elements of the converging intersection (A), the mixing channel (B) in the micro-mixer and the separation channel (C) in the electrophoretic separation system. The arrow indicates the direction of signal flow for microfluidic computation, and subscripts "in" and "out" represent the input and output to the model.

Figures 3A and 3B show the structures of the behavioral models of the converging intersection and the mixing channel (straight or turn) used in a micro-mixer. Different from other elements, converging intersection involves two input streams and one output stream (see Figure 2A). Assume $d^L_{m,in}$ and $d^R_{m,in}$ (m=0,1,2...) are Fourier coefficients of sample concentrations from the left and right input streams respectively, then the output concentration coefficients $d_{n,out}$ are found to be:

$$\begin{aligned} d_{0,out} &= s d^L_{0,in} + (1-s) d^R_{0,in} \\ d_{m\neq 0,out} &= \sum_{m=0}^{m\neq nr} \left\{ 2(-1)^m d^R_{m,in}(1-s) \left(\frac{\cos\left(\frac{F_2}{2}\right)\sin\left(\frac{F_1}{2}\right)}{F_1} + \frac{\cos\left(\frac{F_1}{2}\right)\sin\left(\frac{F_2}{2}\right)}{F_2} \right) \right. \\ &\quad \left. + d^L_{m,in} s \frac{(f_1 \sin(f_2) + f_2 \sin(f_1))}{f_1 f_2} \right\} + \sum_{m=0}^{m=nr} \left(d^L_{m,in} s + d^R_{m,in} (-1)^m (1-s) \right) \end{aligned} \quad (1)$$

where $s = I_L/(I_L + I_R)$ gives the interface position between the streams (I_L and I_R are currents carried by the left and right input streams); $f_1=(m-ns)\pi$, $f_2=(m+ns)\pi$, $F_1=(m+n-ns)\pi$ and $F_2=(m-n+ns)\pi$.

A diverging intersection owns one input and two output streams. The output concentration coefficients can be derived in a similar manner as the converging intersection, but the electric current is partitioned at a ratio depending on the downstream electric resistance.

The mixing straight/turn channel includes one input and one output stream; and the output concentration coefficients $d_{n,out}$ at its outlet are given as

$$d_{n,out} = d_{n,in} e^{-\tau\gamma n^2 \pi^2} \quad (2)$$

where $d_{n,in}$ are the input coefficients at the channel inlet, $\tau = LD/Uw^2$ (L and w are the length and width of the channel respectively; for a turn, $L=R\theta$, where R and θ are the mean radius and angle included by the turn. D and U are diffusivity and electrokinetic velocity of the sample). γ is a factor determined by the cross-sectional shape of the channel. The mixing detector model yields the widthwise concentration profiles (concentration vs. width) of samples, which become important inlet conditions for downstream micro-reactor, if an integrated LOC is considered,

$$C(y) = \sum_{n=0}^{\infty} d_n \cos\left(\frac{n\pi y}{w}\right) \quad (3)$$

where y is the widthwise coordinate of the mixing channel.

Figure 3C shows the structure of the behavioral model of the electrophoretic separation channel (straight or turn). The inherent variable for the functions is the residence time Δt of the analyte band in an element. Δt and amplitude ratio of the band through an element is given as

$$\Delta t = L/E\mu \quad (4)$$

$$A_{out}/A_{in} = \sqrt{\sigma^2_{in}/\sigma^2_{out}} \quad (5)$$

where μ is the electrophoretic mobility of the analyte species in the buffer and other symbols are defined same as the above. To obtain Eq. (5), we always assume a Gaussian concentration distribution for the analyte band in the system. The change of skew coefficients and variance depends on the specific element [11]. For a straight separation channel,

$$B_{n,out} = B_{n,in} \cdot e^{-(n\pi)^2 \Delta t D / w^2} \tag{6}$$

$$\Delta\sigma^2 = 2D \cdot \Delta t \tag{7}$$

For a separation turn,

$$B_{n,out} = \begin{cases} \pm \dfrac{4\theta\left(1-(-1)^n\right)\left(1-e^{-(n\pi)^2 \Delta t D / w^2}\right)}{(n\pi)^4 \Delta t D / w^2} + B_{n,in} e^{-(n\pi)^2 \Delta t D / w^2} & , \ n \neq 0 \\ B_{n,in} & , \ n = 0 \end{cases} \tag{8}$$

$$\Delta\sigma^2 = 2D\Delta t \pm \frac{8w^4\theta}{D\Delta t} \sum_{n=odd}^{\infty} \left(\frac{B_{n,in}\left(1-e^{-(n\pi)^2 D\Delta t / w^2}\right)}{(n\pi)^4} \right) + \frac{64w^6\theta^2}{(D\Delta t)^2} \sum_{n=odd}^{\infty} \frac{\left(-1+e^{-(n\pi)^2 D\Delta t / w^2} + (n\pi)^2 D\Delta t / w^2\right)}{(n\pi)^8} \tag{9}$$

where n=1,3,5... In Eqs. (8) and (9), the plus sign is assigned to the first turn and any turn increasing the skew caused by the first; the minus sign is assigned to any undoing the skew. For the separation detector model, the skew coefficient is transferred without change due to the small detection length L_{det}. The variance associated with the length is given by [4]

$$\Delta\sigma^2 = L_{\text{det}}^2 / 12 \tag{10}$$

The detector model generates an electropherogram (concentration vs. time) when the system is simulated using transient analysis. Spectre will first calculate DC operating points. Based on these points, the transient simulation is then performed by scanning the read-out time. Assuming the band does not substantially spread out as its passes through the detector, we approximate the cross sectional average concentration output (C_m) as

$$C_m = A_{out} \cdot e^{-(E\mu)^2 (t - t_{out})^2 / 2\sigma_{out}^2} \tag{11}$$

where A_{out}, t_{out} and σ_{out}^2 are detector outputs from DC analysis and t is the actual read-out time.

3. RESULTS AND DISCUSSION

Our simulation results for micro-mixers are shown in Figures 4-6 and those for electrophoretic separation systems are given in Figures 7 and 8. Figure 4A illustrates an electrokinetic focusing mixer [5, 6] and its schematic counterpart used in the system simulation. Within the triple-input converging intersection, sample *a* is supplied from the middle input channel and pinched by sample *b* from both side channels, which is followed by mixing in the straight channel. The triple-input intersection is modeled as two serially concatenated double-input converging intersections. In Figure 4B, the simulation results using our behavioral models are compared with the numerical data at two different focusing ratios α (the focusing ratio is defined as $\alpha = I_s / I_i$ and indicates the focusing intensity from the side channels); and an excellent match of relative error less than 3% is found. A high α can drastically reduce the sample bandwidth supplied by the middle channel and accelerate the mixing. Netlisting and DC simulation for this example takes 20 seconds on a multi-user, 2-CPU 1 GHz Sun Fire 280 processors with 4 GB RAM for the first time simulation, and less than a second for subsequent iterations, leading to a 12~250× speedup.

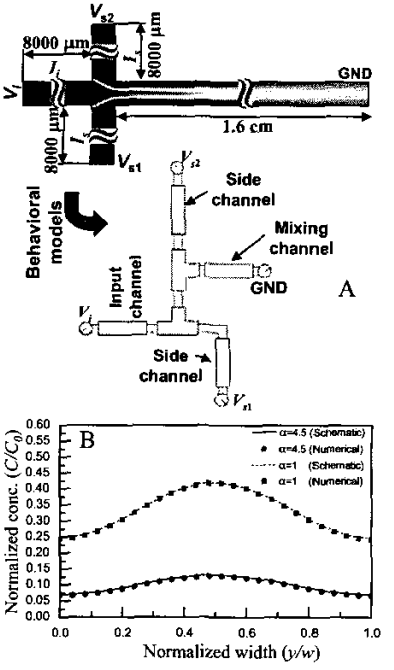

Figure 4. An electrokinetic focusing micro-mixer and its schematic (A) and concentration comparison of numerical data with simulation using behavioral models (B). Properties and parameters used in the simulations are: D=1×10^{-10} m^2/s, μ=6×10^{-8} m^2/(Vs), w=200 μm. For α=4.5, V_i=240 V V_{s1}=V_{s2}=280 V and for α=1, V_i=266.7 V, V_{s1}=V_{s2}=304.8 V.

Figure 5 compares the simulation results on an electrokinetic multi-stream mixer using the schematic in Figure 2A with the numerical data and they agree very well. It is found that at x=0.01L, mixing is achieved at 68% according to the mixing degree, $Q = 1 - \frac{2}{w}\int_0^w |c(y) - c_{avg}| dy$, where c_{avg} is the width-averaged concentration. Over 0.3L<x<L (70% of the channel length), Q is only enhanced from 92%

to 97%. This demonstrates the usefulness of our behavioral models in studying both mixer effectiveness and efficiency.

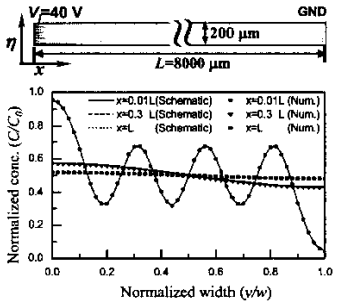

Figure 5. Concentration comparison of numerical data with simulation results using behavioral models of an electrokinetic multi-stream micro-mixer. Properties used in the simulation are: D=1×10^{-10} m^2/s, μ=2×10^{-8} m^2/(Vs).

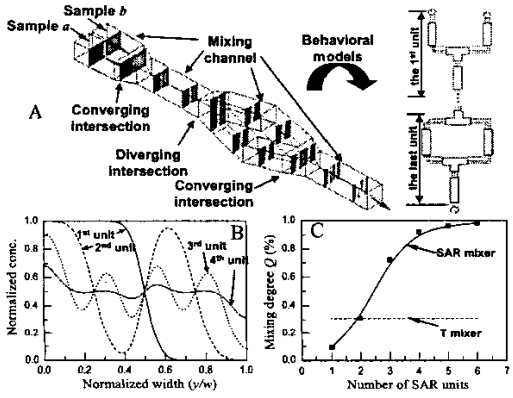

Figure 6. A SAR mixer and its schematic (A) and simulation results of depth-averaged concentration using behavioral models after the 1st, 2nd, 3rd and 4th SAR units (B). The mixing degree Q after each SAR unit, compared to a T mixer (C).

Figure 6A shows a split-and-recombine (SAR) mixer (only the first two units) [9] represented and simulated using the schematic composed by our behavioral models. Different from multi-stream mixer in Figure 5, the SAR mixer performs multi-lamination within the mixer by splitting the stream by a diverging intersection, rotating the streams by 90° and recombining them by a converging intersection. The depth-averaged concentration distributions along the width at the first four SAR units are illustrated in Figure 6B and multiple splitting of the sample layers is clearly observed, which contributes to a tremendous improvement in Q compared with a T-mixer of the same length (Figure 6C). We can also see that the increase in Q is rapid through the first few SAR units and then becomes saturated as sample homogeneity improves. Thus, a tradeoff exists between Q and mixer size, mixing time and system complexity.

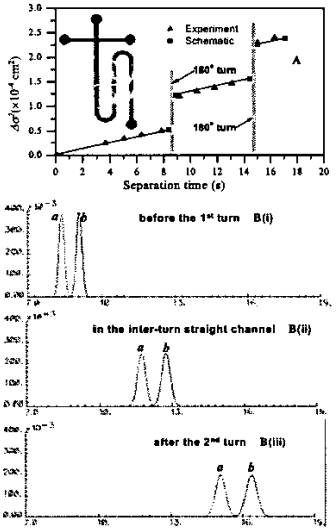

Figure 7. Comparison of experimental data [2] with DC system simulation on a serpentine electrophoretic separation microchip of double complementary turns (A). Transient analysis (B) simulates three detectors' read-outs.

Simulation results using our behavioral models for electrophoretic separation system are shown in Figures 7-8. In Figure 7, a serpentine electrophoresis column of two complementary turns is used to separate an analyte of two species a (D=3.12×10^{-10} m^2/s, μ=1.2×10^{-8} m^2/sV) and b (D=2.72×10^{-10} m^2/s, μ=1.1×10^{-8} m^2/sV). The experimental data [2] of variance growth vs. time on species a is compared to our DC system simulations in Figure 7A, showing an excellent agreement with the maximum relative error of only 5%. Again, netlisting and DC simulation for this example take 20 seconds for the first time and less than a second for subsequent iterations, leading to a 500~10,000× speedup (higher speedup can be obtained when a more complex chip topology or less diffusive species are simulated [11]). The first turn skews the analyte band and accordingly incurs abrupt increase in variance (see the skewed band after the first turn in the numerical simulation plot in Figure 7A). During the analyte's migration in the long inter-turn straight channel, the transverse diffusion smears out most of the skew and presents a nearly uniform band before the second turn. The second turn then distorts the band again in the opposite direction, leading to another turn-induced variance equal to the one caused by the first turn. Figure 7B shows electropherograms of both species from three detectors placed in the system. Respectively their positions are before the first turn, in the inter-turn straight channel and

after the second turn. The spacing between concentration peaks of species *a* and *b* increases as they migrate through the channels; but since both turns broaden the species bands, the amplitude decreases consecutively.

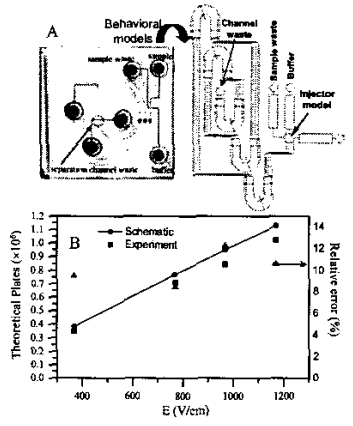

Figure 8. A practical spiral electrophoretic separation system [3] and its schematic counterpart (A); and the comparison of simulation to the experimental data on theoretical plate number vs. electric field. Right axis shows the relative error between simulation and experiments.

In Figure 8, the dispersion of Dichlorofluorescein in a complex spiral separation microchip of five turns is simulated and compared to experimental results [3]. A worst-case error of 12% on plate number N defined as $N = L_{tot}^2 / \sigma^2$ is found, where L_{tot} is the total separation length from injector to the detector. The linear growth of plate number with electric field confirms that molecular diffusion is the major dispersion source in such a system.

4. CONCLUSIONS

Composable system simulation frameworks for both micro-mixers and complex electrophoretic separation systems have been presented, in which parameterized behavioral model libraries using an analog hardware description language (Verilog-A) have been developed. Kirchhoff's law and directional signal flow have been employed to solve the electric and microfluidic network respectively. The system simulation results have been verified by numerical and experimental data. The proposed interface parameters and behavioral models are able to accurately capture the combined effects of system topology, analyte/sample-buffer properties and operational parameters on the mixing and separation performance. Compared with numerical methods, tremendous speedups (12~250× for mixer and 500~10,000× for electrophoretic separation system) can be achieved by simulations using behavioral models, while still maintaining high accuracy (relative error less than 5% for the examples presented in this paper). This enables the sub-hour system-level synthesis and optimal design of these devices. To take advantage of their excellent computational efficiency and accuracy, the behavioral models presented in this paper will be integrated with those of other functional microfluidic components, such as injector and reactor that currently are in progress, to develop an accurate and efficient CAD tool for simulation and design of the entire electrokinetic lab-on-a-chip systems.

5. ACKNOWLEDGMENTS

This research is sponsored by the DARPA and the Air Force Research Laboratory, Air Force Material Command, USAF, under grant number F30602-01-2-0587, and the NSF ITR program under award number CCR-0325344.

6. REFERENCES

[1] Aurouz, P.A., et al., Micro total analysis systems. 2. analytical standard operations and applications. *Anal Chem*, 2002. **74**: p. 2637-2652.

[2] Culbertson, C.T., et al., Dispersion sources for compact geometries on microchips. *Anal Chem*, 1998. **70**(18): p. 3781-3789.

[3] Culbertson, C.T., et al., Microchip devices for high-efficiency separations. *Anal Chem*, 2000. **72**(23): p. 5814-5819.

[4] Jacobson, S.C., et al., Effects of Injection Schemes and Column Geometry on the Performance of Microchip Electrophoresis Devices. *Anal Chem*, 1994. **66**(7): p. 1107-1113.

[5] Jacobson, S.C. and J.M. Ramsey, Electrokinetic focusing in microfabricated channel structures. *Anal Chem*, 1997. **69**(16): p. 3212-3217.

[6] Knight, J.B., et al., Hydrodynamic focusing on a silicon chip: Mixing nanoliters in microseconds. *Phys Rev Lett*, 1998. **80**(17): p. 3863-3866.

[7] Koch, M., et al., Improved characterization technique for micromixers. *J Micromech Microeng*, 1999. **9**(2): p. 156-158.

[8] Reyes, D.R., et al., Micro Total Analysis Systems. 1. Introduction, Theory, and Technology. *Anal Chem*, 2002. **74**: p. 2623-2636.

[9] Schonfeld, F., et al., An optimised split-and-recombine micro-mixer with uniform 'chaotic' mixing. *Lab on a Chip*, 2004. **4**(1): p. 65-69.

[10] Seiler, K., et al., Electroosmotic Pumping and Valveless Control of Fluid-Flow within a Manifold of Capillaries on a Glass Chip. *Anal Chem*, 1994. **66**(20): p. 3485-3491.

[11] Wang, Y., et al. Analytical Dispersion Models for Efficient Simulations of Complex Microchip Electrophoresis Systems. in *Proceedings of Micro Total Analysis Systems*. 2003. Squaw Valley, CA., U.S.A.

[12] Wang, Y., et al. Analytical Models for Complex Electrokinetic Passive Micromixers. in *Proceedings of Micro Total Analysis Systems (Accepted)*. 2004. Malmo, Sweden.

[13] www.cadence.com.